Rapid Automated Materials Synthesis Instrument: Exploring the Composition and Heat-Treatment of Nanoprecursors Toward Low Temperature Red Phosphors

Tian Lin,[†] Suela Kellici,[†] Kenan Gong,[†] Kathryn Thompson,[†] Julian R. G. Evans,[†] Xue Wang,[‡] and Jawwad A. Darr*,[†]

Christopher Ingold Laboratories, Department of Chemistry, University College London, 20 Gordon Street, London WC1H 0AJ, United Kingdom, and Institute of Particle Science & Engineering, School of Process, Environmental and Materials Engineering, University of Leeds, Clarendon Road, Leeds LS2 9JT, United Kingdom

Received July 24, 2009

We report on the commissioning experimental run of the rapid automated materials synthesis instrument (RAMSI), a combinatorial robot designed to manufacture, clean, and print libraries of nanocrystal precursor solid compositions. The first stage of RAMSI, parallel synthesis, uses a fully automated high throughput continuous hydrothermal (HiTCH) flow reactor for automatic metal salt precursor mixing, hydrothermal flow reaction, and sample slurry collection. The second stage of RAMSI provides integrated automated cleanup, and the third section is a ceramic printing function. Nanocrystal precursor solid ceramics were synthesized from precursor solutions and collected into 50 mL centrifuge tubes where they were cleaned by multiple centrifugation and redispersion cycles (monitored by intelligent scanning turbidimetry) and printed with an automated pipette. Eight unique compositions of a model phosphor library comprising pure nano-$Y(OH)_3$ and Eu^{3+} doped-yttrium hydroxide, $Y(OH)_3$:Eu^{3+} nanocrystal precursor solid were synthesized (with 2 centrifuge tubes' worth collected per composition), processed, and printed in duplicate as 75, 100, and 125 μL dots in a 21.6 ks (6 h) experiment (note: the actual time for synthesis of each sample tube was only 12 min so up to 60 compositions could easily be synthesized in 12 h if one centrifuge tube per composition was collected instead). The $Y(OH)_3$:Eu^{3+} samples were manually placed in a furnace and heat-treated in air for 14.4 ks (4 h) in the temperature range 200−1200 at 100 °C intervals (giving a total of 84 samples plus one as-prepared pure $Y(OH)_3$ sample). The as-prepared and heat-treated ceramic samples were affixed to 4 mm wide hemispherical wells in a custom-made aluminum well-plate and analyzed using a fluorescence spectrometer. When the library was illuminated with a 254 nm light source (and digitally imaged and analyzed), the 3 mol % Eu^{3+} sample heat-treated at 1200 °C gave the most intense fluorescence (major red peak at 612 nm); however, an identical nanocrystal precursor heat-treated at only 500 °C (identified as Y_2O_3:Eu^{3+} after heat treatment) was the brightest phosphor under illumination of the samples heat-treated at or below 1000 °C.

Introduction

Nanochemistry concerns the syntheses of sub-100 nm diameter particles with different sizes, shapes, compositions, surface structures, and functionalities with applications such as components of solar cells,[1] high efficiency fuel cell materials,[2] active gas sensors,[3] and fine chemical catalysts.[4] Nanomaterials can generally be synthesized by either top-down (e.g., comminution) or bottom-up (molecules to nanoparticles) approaches.[5] Many nanomaterials syntheses are time and energy consuming and give inconsistent results with batch to batch variations. Faster and more consistent nanomaterials synthesis and processing methods are highly desirable.

Combinatorial techniques are used where predictive theory is weak, and they allow a large number of samples to be prepared and characterized rapidly, some of the earliest efforts being made in the fields of organic chemistry, drug design, and biotechnology.[6,7] The arena of combinatorial materials development is rather more recent and include the fabrication of addressable solid state materials libraries via thin film deposition and physical masking techniques.[8] More recently, one of the authors previously developed a fully automated combinatorial robot (London University Search Instrument: LUSI),[9−11] capable of printing combinatorial libraries from commercial ceramic powders using adapted inkjet printers and then sintering them in a multizone furnace at up to 1600 °C. Others recently developed a fully automated combinatorial robot[12−14] using a functional modular approach based on a conventional solid state reaction which prepares inorganic powders in air, from weighing and mixing of starting materials to processing the compounds in a

* To whom correspondence should be addressed. E-mail: j.a.darr@ucl.ac.uk.
[†] University College London.
[‡] University of Leeds.

10.1021/cc9001108
Published on Web 04/26/2010

furnace.[15] Combinatorial ceramic libraries have also been made using other top-down approaches.[16] Such methods usually start with metal oxide precursors, and involve metering, mixing, and firing of such mixtures possibly with a printing step.[17] This is often followed by automated analyses of libraries using techniques such as automated powder X-ray diffraction (XRD).

One of the limitations of starting with metal oxide powders for heterometallic solid state chemistry[18] is that atom diffusion may be insufficient to achieve equilibrium phase composition (hence, intermittent calcining and grinding steps are often used which are difficult to automate). This limitation can often be overcome by use of a bottom-up strategy[19] that employs inherently smaller diffusion distances. Such approaches have been applied to the syntheses of catalyst powders and thin-film preparation of complex inorganic materials (e.g., electronic, optical, luminescent, magnetic and catalytic materials) by masking techniques coupled with laser deposition.[9,10,20,21] Bottom-up methods usually produce libraries which can be heat-treated if required to bring about solid state chemical transformations which makes them effective for the preparation of gradient mixture libraries.

In recent years, continuous hydrothermal flow synthesis (CHFS) reactors have been used to rapidly and efficiently produce nanoparticles from atomically mixed metal salt solutions which react with a flow of supercritical water at typically 450 °C and 22 MPa in a reactive mixer (in seconds).[22−32] The formation reaction of metal oxide nanoparticles from metal salts (e.g., nitrates) usually follows a two step mechanism, with hydrolysis rapidly followed by dehydration[23] and usually some decomposition (not shown below) of the anions:

$$\text{Hydrolysis:}\quad M(NO_3)_x(aq) + xH_2O \rightarrow M(OH)_x(s) + xHNO_3 \quad (1)$$

$$\text{Dehydration:}\quad M(OH)_x(s) \rightarrow MO_{x/2}(s) + (x/2)H_2O \quad (2)$$

More recently, the authors reported a significant development of the CHFS reactor known as a high throughput continuous hydrothermal (HiTCH) flow synthesis reactor[33] which produces many nanoceramic samples sequentially in a few hours. Despite being a manual apparatus, the HiTCH flow synthesis reactor was used to make a 66-sample nanoparticle library (ternary phase diagram) of nanocrystalline $Ce_xZr_yY_zO_{2-\delta}$ in less than 43 ks (12 h).[33] Samples were then cleaned manually by repeated centrifugation and redispersion in clean water until a fixed amount of supernatant had been exchanged. Despite this huge advance in nanomaterials preparation, the HiTCH flow synthesis process required considerable human operational effort. In this regard, automation of the entire HiTCH flow synthesis process from individual metal salt (precursor) mixing to nanoparticle synthesis, collection and automation of cleanup (and printing if possible) would be highly desirable and reduce the possibilities for human error.

Herein, we report the results of the first operational run of a new and flexible nanomaterials synthesis robot, the rapid automated materials synthesis instrument (RAMSI). Metal salts were automatically mixed and introduced into an automated HiTCH flow synthesis system and then collected as slurries. The sample cleanup and printing of samples as dots in RAMSI (using a robot arm) and carousels (motorized and pneumatic manipulators) to handle samples, is also described. The system works with multithreading and multitasking programs and makes intelligent judgments during sample processing to operate efficiently.

Instrument Design. The model codes and sources of components used in construction are given in the Supporting Information, Supplementary text S1; other items were custom-built in-house. The control automation within RAMSI was largely built by Labman Automation (Stokesley, U.K.) under contract and according to a collaborative design

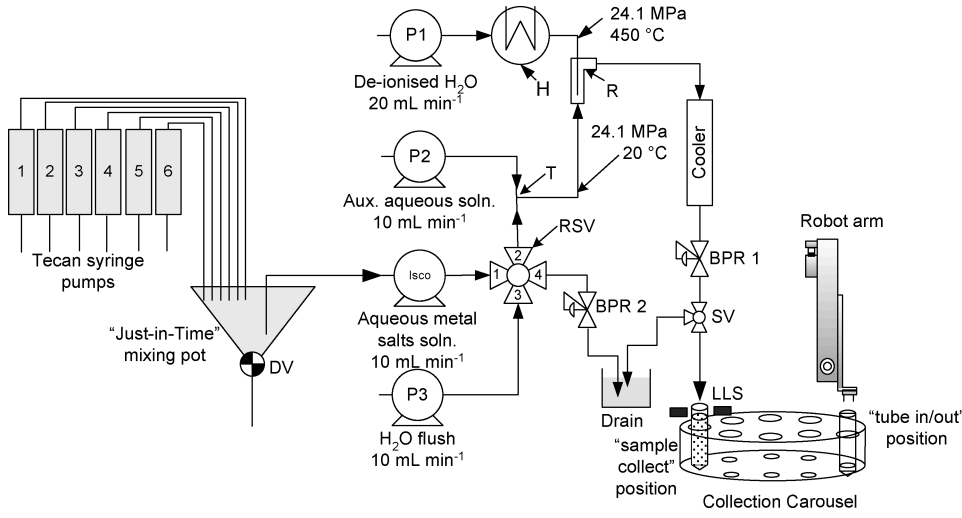

Figure 1. Schematic representation of the synthesis and collection part of RAMSI that was used to prepare the phosphors library. Key: P = Gilson pump, Isco = Isco syringe pump, H = heater, R = counter-current mixer, T = T-piece, RSV = Rheodyne switch valve, BPR = back-pressure regulator, DV = drain valve, SV = two way switch valve, LLS = liquid level sensor. Each high pressure line also contains non return valves, pressure relieving safety devices, electronic pressure transducer, and manual pressure gauges which are not shown here for clarity.

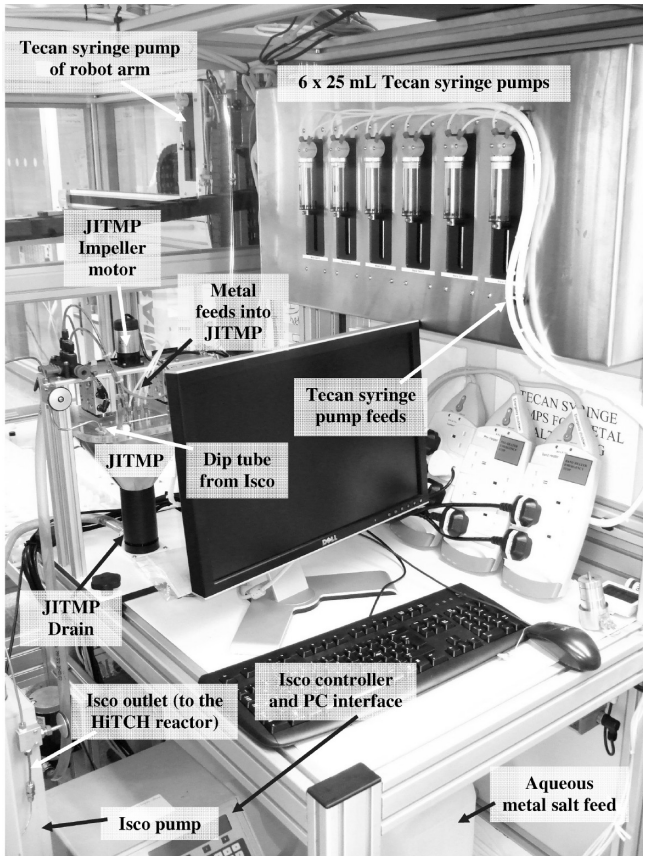

Figure 2. Photograph of the right-hand side of the synthesis part of RAMSI showing the bank of 6 × 25 mL Tecan syringe pumps and their feeds and the custom built "just-in-time" mixing pot (JITM).

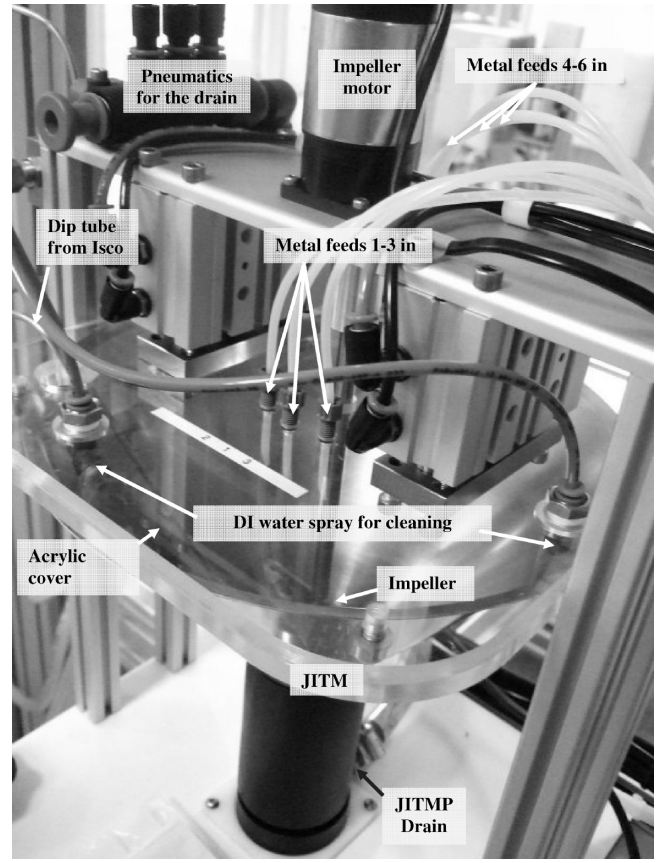

Figure 3. Photograph of the custom built "just-in-time" mixing pot (JITMP) which is located in the synthesis section of RAMSI showing metal salt feeds (from the 6 × Tecan Syringe pumps), the JITMP drain, JITMP impeller used to mix the metal salts and a dip tube from the Isco syringe pump which removes mixed metal salts in order to deliver them to the hydrothermal reactor.

process with the authors. The operational scheme for the synthesis and collection sections of RAMSI is shown in Figure 1. In Figure 1, six Tecan syringe pumps each equipped with a 25 mL barrel (dispensing resolution 100 μL) were used for volumetric metering of the source metal salt solutions into a "just-in-time" mixing pot (JITMP) which was equipped with stirrer and drain (see photographs in Figure 2 and 3). An Isco syringe pump was used to draw from the mixing well and inject into the HiTCH flow synthesis reactor via a Rheodyne switch-valve (RSV) while simultaneously diverting cold water from HPLC pump P3 to the drain via BPR2, as shown in Figure 1. Gilson HPLC pumps and injectors were used to deliver water to the superheated and flushing streams.

The water heater (H in Figure 1), controlled by a digital controller and temperature limit controller provided the superheated feed. A 2.5 kW electrical water preheater was built from 1/4″ fittings and consisted of a 1 kW cartridge heater enclosed in an aluminum cylinder around which 6 m of 1/4″ stainless steel high pressure tube was wound. The whole preheater assembly was then surrounded with a custom-made Watlow heater jacket (1.5 kW). A small 50 mm long, 200 W band-heater was used to maintain temperature at the mixing point (R in Figure 1).

The new automated HiTCH flow synthesis reactor[33] was built on a mobile (wheeled) frame to allow it to be removed for maintenance (Supporting Information, Figure S1a and S1b). The reactor was one of a pair of reactors which allowed the operator to run one reactor while the other underwent maintenance. Pressure monitoring and control made use of a 40 MPa pressure gauge, pressure release safety valves (set to 29 MPa), Swagelok non-return valves, two electronic pressure transducers connected to digital displays, and two back pressure regulators (BPR1 and BPR2). The exit of the back-pressure regulator from the HiTCH flow synthesis reactor included a ball valve operated by a pneumatic actuator (Supporting Information, Figure S2).

The collection carousel (full photograph in Supporting Information, Figure S2) consisted of an encoded stepper motor driving a circular rack of centrifuge tubes and a level indicator sensor to ensure the tubes were filled with nanocrystal precursor slurries to 50.0 mL ± 0.9 mL (Figure 4). The choice of 50 mL centrifuge tubes was dictated by the need to produce at least 100−300 mg typically to get enough sample and by the concentrations used (to minimize the opportunity for blockages). This amount of sample per tube was also ideal as it enabled libraries to be made of samples which could be readily analyzed using the automated analytical equipment at UCL (XRD, Raman, etc.).

The robot arm (Figure 5) had a total movement space of 2400 × 1040 × 560 mm in the *x*-*y*-*z* directions inside an enclosure with approximate dimensions 3330 × 2500 × 1800 mm. All the robot axes were stepper motor driven. The *x*-*y*-*z* motion robot arm incorporated a custom-built, four pin, centrifuge tube gripper driven by a pneumatic actuator

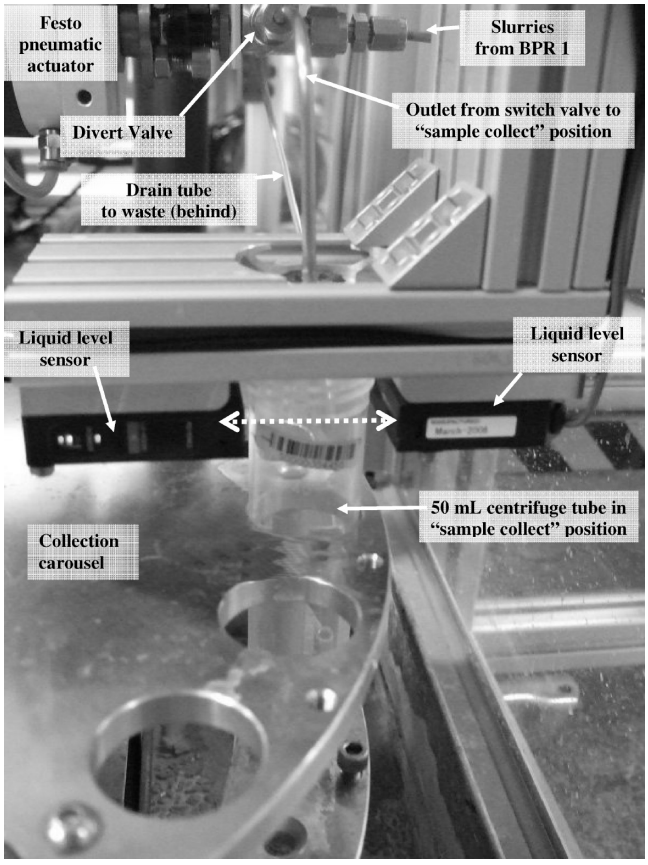

Figure 4. Photograph showing the collection carousel in the "sample collect" position and level indicator sensor ensuring the centrifuge tubes are filled to 50.0 mL.

(shown in Figure 5 holding a 50 mL centrifuge tube) and a custom-built tip loader (which used a Tecan syringe pump with a 5 mL barrel) suitable for picking and printing from standard 5 mL Eppendorf pipette tips in a rack.

The cleanup and printing sections[34] made use of equipment described in the Supporting Information, Supplementary text S1 (also see Supporting Information, Figure S3 showing the relative layout of the synthesis, collection, cleaning, and printing areas in RAMSI). The cleanup section had a total rack capacity for 288 (50 mL) centrifuge tubes (total of four centrifuge tube racks), 28 centrifuge tubes at a time in each robot centrifuge (7 tubes $\times$4 holders) and at least 120 pipette tips (60 tips $\times$2 racks).

Control Software and Protocols. For compatibility with the various device protocols, VB.NET was chosen as the development tool. It also allows flexibility in customer tailored functions by manipulating device firmware. Adoption of multithreading and multitasking techniques provides potential expansion in production capability. Design of user interfaces and a production database also took into account future development, for example, data link to a materials database developed in MySQL. The key issue for multithreading in RAMSI[35] is to avoid potential conflicts between the threads when they share devices or operations. Technically, the program solved this by keeping precise and strict logs of status for each thread. Perfect coordination was set up among the parallel threads by intelligently judging the status. Three threads, mixing, injection, and reactor (including collection) were run in parallel and coordinated. Our preliminary trials proved that this multithreading strategy could make 48 samples within 29 ks (8 h) with 1 tube collected for each sample, and the authors envisage further improvements can be made in the future. Multithreading allowed the Isco syringe pump to be purged after each injection by implementing diversions and was used for the cleanup section, particularly the cleanup carousel and robot arm motions to minimize travel distances and eliminate the possibility for crashes.

Four categories of communication protocols were integrated within RAMSI.[35] These were (i) serial communication, (ii) dedicated control adaptor with manufacturer-supplied software module (e.g., the robot arm and supernatant scan axis driven by a motor control card), (iii) digital signal, and finally (iv) ethernet connections, for example, barcode reader (the latter is not operational at time of writing). All these were integrated on a PC platform by VB.NET which allows more instruments to be added to enhance analytical capability.

Alarm and emergency-stop procedures were integrated into the software. The synthesis software module has a fourth thread dedicated to real-time status monitoring with a sampling period of 1 s and includes safety limits for preheater temperature and reactor pressure. The "operation limits" confirms whether reactions take place under accepted tolerances, and exceeding the set pressure or temperature safety limits initiates an emergency stop procedure providing alerting messages, visual and audible alarms, and shut down of power to the preheater core and band heater.

Running Sequence. The synthesis began by running the HPLC pumps (pumps P1−P3 as shown in Figure 1) and switching the heaters on to get the reactor up to temperature. Each metal salt was delivered to the JITMP by the Tecan syringe pumps and the mixed solution aspirated into the Isco pump thence through ports 1 and 2 in the RSV to then meet a KOH (base) solution feed from pump P2 at a 'T'-piece (T in Figure 1). This mixture under flow confronted superheated water in the counter-current mixer (R in Figure 1) at which point nucleation and growth of particles took place. After passing through the cooler, the suspension emerged through a back-pressure regulator (BPR1 in Figure 1) and then through a diverting valve which can switch the output between "collection" and "drain". The HiTCH reactor initially received 15 mL of each mixed metal salt solution (first injection) which ran through it and was rejected to the waste as a purge (out via BPR2 in Figure 1). The remaining 27 mL of the same mixed metal salt solution (second injection) was also fed into the reactor (after mixing with the base solution) and met the superheated water feed and exited from BPR1 (Figure 1). A 100 mL portion of the resulting slurry was collected in two centrifuge tubes (2 $\times$ 50 mL), and an optical level sensor was used to detect a full tube (Figure 4). At this point the slurry flow was momentarily diverted (via a pneumatically operated divert valve) to a waste drain in the interval needed for the second tube to rotate into the collection position in the collection carousel. The HiTCH reactor was then purged between consecutive compositions by diverting clean water from pump P3 toward the reactor R for 120 s using the RSV. In parallel, the JITMP

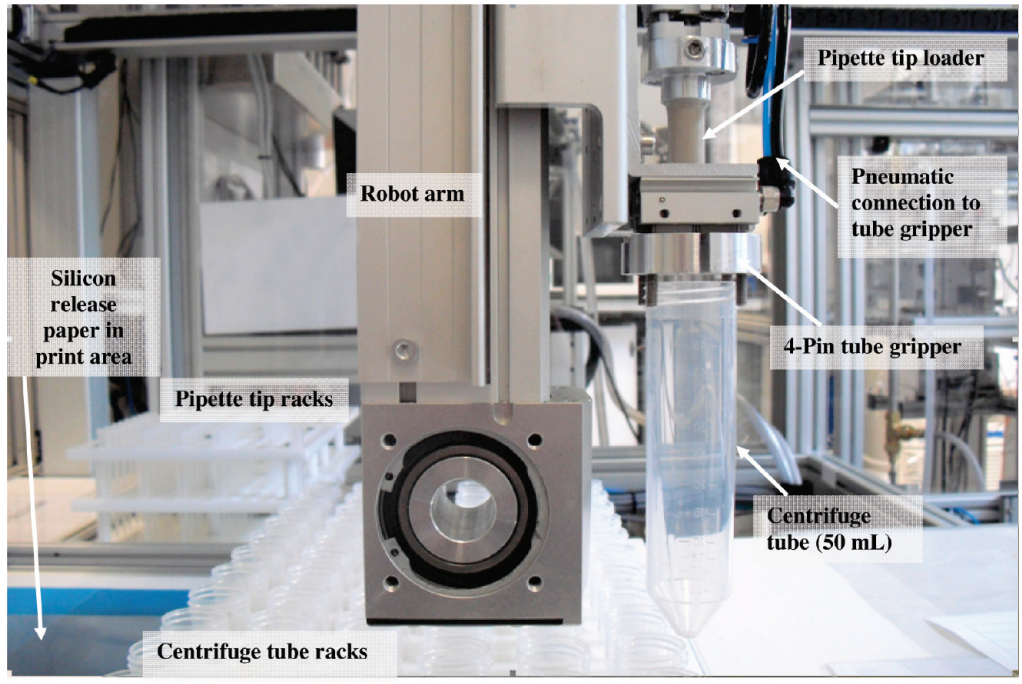

Figure 5. Photograph showing the robot arm which incorporates a 4-pin tube gripper (for moving 50 mL centrifuge tubes) and behind it is the pipettor which accommodates a 5000 μL pipette for printing slurries onto the hydrophobic silicon release paper which reduces wetting of the slurries. The pipette tip and 50 mL centrifuge tube racks are also shown.

was purged with 300 mL of clean DI water, and the Isco syringe pump was then purged with three washes of clean DI water (50, 30, and 30 mL) from the JITMP.

After all syntheses had been completed, the cleanup process began. Counter ions were removed in the cleanup process[34,35] as follows: the slurry-filled centrifuge tubes were placed by the robot arm into the 28 slot automated centrifuge located in the cleanup area and spun at 4500 rpm for 30 min. After this, they were taken to the fixed turbidimetry station one at a time to ascertain if they were clear enough for 10 mL of clean liquid to be removed. Any samples that passed were then placed into the cleanup carousel, and the liquid was removed by a needle attached to a scanning turbidimetry sensor. Samples were partially topped up to 40 mL with clean DI water, and the sediment was redispersed using an automated high shear mixer (includes associated wash station).[34,35] Finally, the contents of each tube were made up to 50 mL, and the tubes placed back into the centrifuge. The entire process was repeated for a further three times until a total of 135 mL had been replaced for each tube. In the final cleanup cycle, 45 mL of liquid was removed to leave a concentrated slurry (such a cleanup gave a theoretical maximum K^+ concentration in the solid product of 18 ppm). Each unique composition was combined into one centrifuge tube using the pipette on the robot arm. The samples were further concentrated to ~45 wt % solids by allowing them to evaporate slowly in air for a further 12 h.[34,35]

The robot arm pipettor autoloaded a 5000 μL tip for each sample (and discarded a tip after each sample) and aspirated slurries from the tubes to print dots of a set number and size on hydrophobic silicone paper.[34,35] These samples were later manually assembled into a custom-made 96 well (86 × 123 mm) solid aluminum well-plate library with 4 mm wide, 1.5 mm deep wells (9 mm between the center of each well) as shown in Figure 6a.

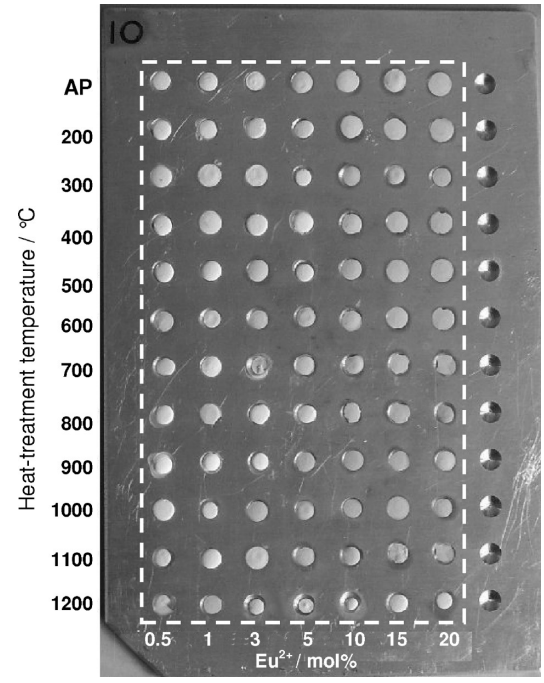

Figure 6. Photograph of the library under daylight. Samples were made in the automated HiTCH flow synthesis system of RAMSI using a superheated water flow at 450 °C and 24 MPa, dried in air as ceramic dots and heat-treated in air for 4 h at a temperature in the range 200−1200 °C (at 100 °C intervals). The ceramic dots were embedded flat side up into a custom-made aluminum plate library using PVA glue.

Experimental Details

The source materials, [$Y(NO_3)_3 \cdot 6H_2O$, (99.9%)] and nitric acid (technical grade, 69%) were supplied by Sigma-Aldrich

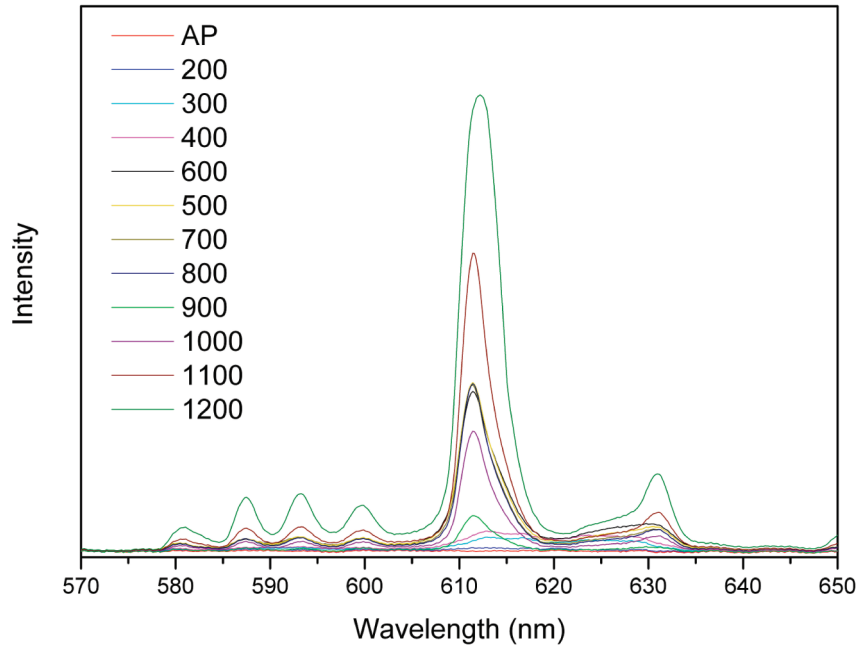

Figure 7. Photoluminescence (PL) emission spectra for 3 mol % Y_2O_3:Eu^{3+} sample heat-treated at a range of temperatures between 200−1200 °C. The sample heat-treated at 1200 °C showed the highest PL intensity.

Chemical Co. (Dorset, U.K.). Eu_2O_3 (99.9%) was kindly gifted by AMR Europe (Abingdon, U.K.). KOH pellets (≥85%) were supplied by VWR International (Leicestershire, U.K.) and used to adjust pH. All experiments were conducted using deionized water (10 MΩ). A 0.2 M solution was made by accurately weighing $Y(NO_3)_3 \cdot 6H_2O$ (26.81 g, 0.07 mol) and adding deionized water to a final volume of 350 mL. Separately, Eu_2O_3 (2.46 g, 0.007 mol) was dissolved in 1.5 mL of 69% nitric acid and then diluted with 33.5 mL deionized water (0.2 M concentration). Thereafter, the desired mole ratios of the 8 compositions of pure $Y(OH)_3$ and Eu^{3+} doped $Y(OH)_3$ (known hereafter as $Y(OH)_3$:Eu^{3+}) with nominal compositions of 0.5, 1, 3, 5, 10, 15, and 20 mol % dopant, were entered into the GUI interface of RAMSI. Thus, two of the six available Tecan syringe pumps were used for volumetric mixing of Y^{3+} and Eu^{3+} solutions.

The $Y(OH)_3$:Eu^{3+} samples were cleaned up,[34] and concentrated slurries were printed as 75, 100, and 125 μL dots (in duplicate) and allowed to air-dry on silicone paper.[34] All the ceramic dots except one composition (pure $Y(OH)_3$ not shown) formed a dome shape. A sample dot from each doped composition was heat-treated in air for 14.4 ks (4 h) on a solid platinum plate in the range 200−1200 at 100 °C intervals using a programmable furnace at a heating and cooling rate of 0.17 °C s^{-1} (10 °C min^{-1}). Samples were obtained as well−formed, printed dots which were white in color. Photoluminescence spectra of selected samples (see Figure 7 for the stacked spectra for the as-prepared and heat-treated 3 mol % Eu^{3+} doped $Y(OH)_3$ samples) were measured using a Cary Eclipse spectrometer (Varian, Oxford, U.K.) fitted with a fiber optic accessory. The entire 84 sample library (which excludes the pure Y_2O_3) was illuminated with a multiband UV light whose peak emission was at 254 nm, and a fluorescent image was captured (Figure 8a) using 10.0 megapixel BENQ digital camera (model DC E1050, Dixons, London, U.K.). The intensity information from the digital image was extracted using MATLAB (impixel function) to obtain the RGB values of a representative central pixel of each illuminated ceramic dot. The extracted RGB and corresponding intensity values are supplied in the Supporting Information, Table S1 and shown as a contour plot in Figure 8b (with z axis as intensity).

Results and Discussion

RAMSI was designed and built during a 3 year period from October 2006 in which time the authors first investigated the most efficient method possible to increase throughput of a continuous hydrothermal flow reactor. Many designs were attempted to try and achieve this, with the major purpose being to increase throughput, eliminate contamination, allow flexibility in sample size, and have complete automation of not only synthesis but also cleanup and printing (which are the most laborious functions). The authors concluded from several months of testing/experimentation that a parallel approach to synthesis using continuous hydrothermal flow reactor systems would have been very complex to monitor, and would have been difficult to operate while ensuring continuous and safe maintenance of high temperature and pressure. From our early work, the HiTCH flow synthesis reactor was developed[33] which was a manual system but it could allow several samples to be made in a day at a fixed sample size. Indeed, a recent report by the authors described the use of the HiTCH flow synthesis reactor for fabrication of 66 unique sample compositions.[33] In the HiTCH system of RAMSI the counter-current mixer (where particles are formed) was similar in size to that used in existing laboratory CHFS reactors which meant that any promising materials from RAMSI could immediately also be made up to 100 g per day quantities via CHFS if required in the future.

A major task in this work was to automate the HiTCH system while making it very flexible in terms of sample size.

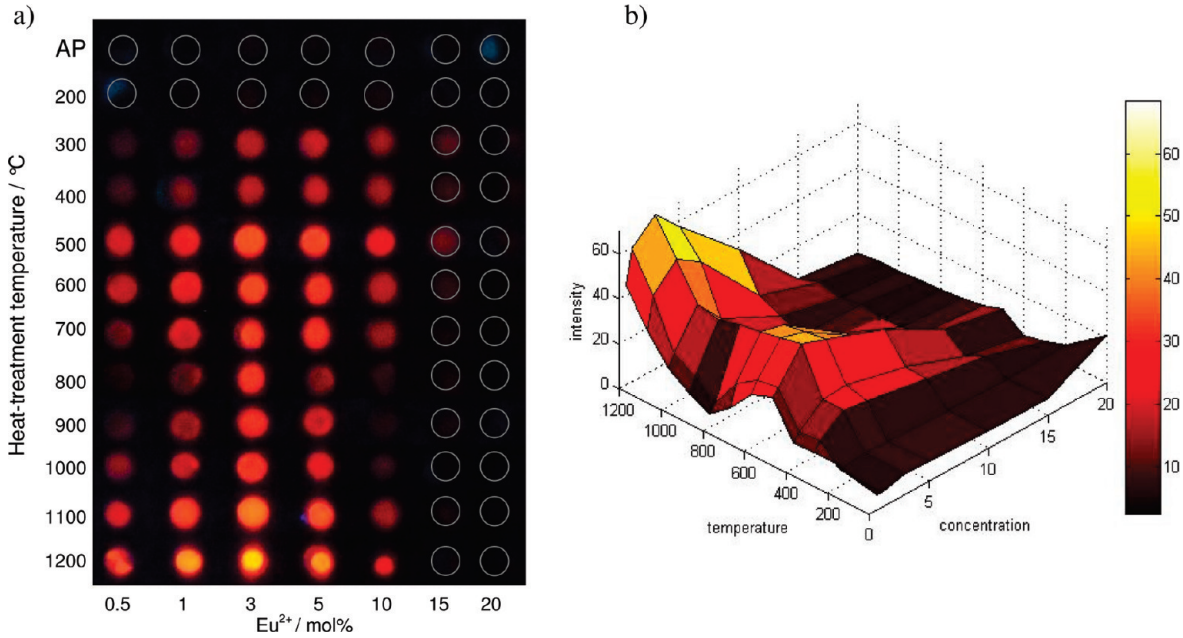

Figure 8. (a) Photograph of the library under UV light illumination (254 nm) showing the changes in intensity with heat-treatment temperature and Eu^{3+} mol % (AP = as prepared sample with no further heat-treatment). (b) A contour plot showing the extracted image intensities (arbitrary units on *z* axis) from the photograph versus heat-treatment temperature (°C) and Eu^{3+} dopant concentration in yttria (mol %). The plot suggests a gradual change of properties exists and that the most intense phosphor at lower temperatures is the 3 mol % Eu^{3+} sample heat-treated at 500 °C, while the brightest sample was the same sample composition heat-treated at 1200 °C.

The authors decided that as RAMSI was to incorporate cleanup, each sample size would be according to increments of how many centrifuge tubes per sample composition were required. When we were deciding on the size of samples, we had to be able to produce enough sample in a basic 50 mL centrifuge tube (order of a minimum of 100−300 mg, depending on reaction) to allow multiple dots to be made so that the authors had the option to potentially carry out heat-treatments on several dots of each composition and that these dots would be big enough (a few mm in diameter) to be analyzable via in-house automated analytical apparatus (such as XRD, Raman and Fluorescence spectrometers, etc.) using wellplates. Additionally, the system was required to produce multiple 50 mL tubes per sample, in order to produce quantities of around 1 g per sample for potential future tests, for example in photocatalysis testing. RAMSI was thus designed to be able to accommodate single or multiple tube sample production.

Hence, the development of RAMSI involved not only complete automation of the original HITCH process, but also several major design innovations. These include the automated metal salt mixing, allowing automatic introduction of the mixed metal salts (with a variable volume at high pressure) into a high pressure flow reactor. This was solved by use of an Isco high pressure syringe pump which could be self-cleaned during the process as required. The Isco pump allowed production of any size of mixed metal salt solution up to 260 mL, where previous HiTCH work was limited by injection loop size to a maximum of 2 mL. As outlined above, the high throughput cleanup and printing parts of RAMSI via turbidimetry scanning as described is completely original in this context as far as we are aware. Some aspects of the process required human interaction such as the drying of concentrated slurries to ensure that the ceramic dots were printable as to form sound uncracked disks where possible on the silicone paper. Also samples were manually embedded into the aluminum wellplate to ensure sample quality for analysis.

In this commissioning run, the fully automated materials synthesis robot RAMSI was used to produce printed dots of pure $Y(OH)_3$ and $Y(OH)_3$:Eu^{3+} ceramics (made in duplicate) with nominal Eu^{3+}content of 0.5, 1, 3, 5, 10, 15, and 20 mol %, which after heat-treatment gave a total of 84 doped samples (not including the pure yttria). The total time of 6 h includes all time for cleaning and printing (assuming it happened in sequence for the same samples). As stated above, these tasks can be done in parallel if required, that is, if a previous sample batch has been made, it can be cleaned while new samples are made. Within the 6 h it only took 1.6 h to make 16 centrifuge tubes full (2 tubes for each of 8 samples). This equates to a throughput of 12 min or so per sample tube. Our preliminary trials proved that this multithreading strategy could make 48 samples within 29 ks (8 h) with 1 tube collected for each sample, and the authors envisage further improvements can be made in the future. In this case, two tubes per sample were made (to be cautious and to have enough sample); however, we envisage in most of the high throughput research in the future that one sample tube per composition will be more than enough sample to carry out analyses (this is obviously application dependent to some degree). This is a substantial saving of as much as 5 to 50× throughput compared to a batch hydrothermal process which is an inferior (from process control point of view) but more common alternative.

The entire 84 sample library was irradiated with a multiband UV lamp at a peak wavelength of 254 nm, the digital photograph of which is shown in Figure 8a. The authors felt that comparison to a commercial phosphor within

this library was not a worthy exercise because commercial phosphors differ wildly in dopant concentration and purity and are strongly affected by crystallite size and synthesis conditions and history. From the photograph of the library under illumination it can be seen that weak photoluminescence was observed for the 3 mol % Eu^{3+} doped $Y(OH)_3$ nanocrystal precursor solid sample heat-treated at 400 °C for 14.4 ks (4 h). However, the same $Y(OH)_3$:Eu^{3+} solid sample showed significantly increased fluorescence intensity when heat-treated at 500 °C (Figure 8b) because of the formation of Y_2O_3:Eu^{3+} (as expected from the literature and from our XRD evidence, see Supporting Information, Figure S4). In particular, the 3 and 5 mol % doped phosphors showed the highest PL intensity among all the samples tested. Interestingly, from the photo, the fluorescence intensity seemed to reduce again as the heat-treatment temperature was increased beyond 500 °C and up to 1000 °C despite the fact that the samples are not changing phase[37] (Supporting Information, Figure S4). A sudden increase in PL intensity was then observed for samples heat-treated at 1200 °C (giving the brightest phosphor in this case: Figure 8b).

The room temperature PL spectra of 3 mol % doped samples (from $Y(OH)_3$:Eu^{3+} to Y_2O_3:Eu^{3+} depending on the temperature of heat-treatment) are shown in Figure 7 (Supporting Information, Figure S5 for the 5 mol % sample also). In general, the emission spectra of Y_2O_3:Eu^{3+} (formed at 500 °C and above) gave rather broad peaks under 254 nm excitation consisting of red emission peaks at 581 (corresponding to $^5D_0$-$^7F_0$), 587, 593, 600 (corresponding to $^5D_0$-$^7F_1$), 612 nm (highest intensity and asymmetric peak corresponding to $^5D_0$-$^7F_2$ transition with Eu^{3+} ions) and 630 nm (corresponding to $^5D_0$-$^7F_3$ transition).[36,38] No monoclinic phase was suggested from the PL spectra because of the absence of any high intensity $^5D_0$-$^7F_2$ emission peak at 623 nm.[39] From the PL spectra, the highest intensity spectrum corresponded to composition 3 mol % Eu^{3+} for the solid heat-treated at 1200 °C (which had Y_2O_3:Eu^{3+}), which was consistent with initial observations obtained from the photoluminescence photograph (although the photograph and PL spectra do not precisely follow the same rank ordering of PL intensity thereafter). The general trend (in decreasing order) of peak intensities for the peak at about 612 nm in the PL spectra (3 mol % Eu^{3+}) was 1200, 1100 and 500, 600, 700, 800 (all four similar), then 1000, 900 and 400, 300, and 200 °C (last three are virtually no peak), while the order for the image intensities from the image analysis was 1200, 1100, 500, 600, 700, and 900, 800, 1000 (three quite similar), then 400, 300, and 200 °C. It should be noted that although there is not much difference in the intensities for some of the samples, the image analysis was successful in identifying trends and areas of very low and very high PL intensity, in a relatively short time.

The optimal doping level depends on many factors including synthesis method, size of the particles, post-treatment temperature, and the existence of segregated phases. The lack of strong fluorescence in the as-prepared materials or those heat-treated at <500 °C is due to the material being $Y(OH)_3$:Eu^{3+} which does not fluoresce appreciably. It is interesting to observe that the 3 mol % $Y(OH)_3$:Eu^{3+} nanocrystal precursor solid sample subjected to a low temperature heat-treatment of only 500 or 600 °C showed substantial PL intensity (because of formation of Y_2O_3:Eu^{3+}). It should be said that the thermal phase transformation from the doped hydroxide to the oxide under these conditions is however expected on the basis of numerous reports in the literature and XRD analysis (Supporting Information, Figure S4). The high brightness of the sample heated to only 500 or 600 °C was very promising as such materials normally require in excess of 1200 °C to show similar properties (sample at 500 °C was the seventh brightest phosphor in Figures 8a and 8b according to image analysis).[40−42] This suggests the material (3 mol % at 500 °C) is relatively crystalline despite the small crystallite size of about 8 nm based on application of the Scherrer[43] equation to the (222) peak of the relevant powder XRD pattern. There is an apparent slight reduction of PL intensity of selected samples heat-treated between about 800 and 1000 °C (Figure 8a and 8b) which corresponds to the onset of atom mobility for all samples and may be associated with neck-growth and sintering of crystallites or indeed with minor adjustments of stoichiometry as the oxide begins to equilibrate with ambient p_{O_2}. Hence, Figure 8b suggests that the sample heat-treated at 500 °C (Y_2O_3:Eu^{3+} with 3 mol % dopant) has a local maximum intensity rather than a global maximum in these 84 samples. This "double hump" contour plot in Figure 8b seems to be novel as phosphors normally display a steady increase in brightness with heat-treatment temperature up to an optimum value (usually ca. 1100−1200 °C). In this context, the use of a digital image is of course reliant on the sensitivity of the camera to the particular PL wavelength, but as an initial screen it provides rapid and convenient mapping behavior to identify regions for further investigation (such data can be a precursor to more detailed analyses such as determination of quantum efficiencies, PL spectra, etc.). Furthermore, it is likely that with the addition of known intensity calibration, the image analysis measurements may be more meaningful in the future.

In the literature, there are various optimum doping levels reported ranging from 4−10 mol % Eu^{3+} in Y_2O_3:Eu^{3+}.[43−46] The differences within the literature and to our results may partly be due to differing levels of homogeneity between different materials, with a suggestion that the materials produced herein are extremely homogeneous because of the speed of precipitation and rapid crystallization for samples made in HiTCH flow synthesis and CHFS reactors despite the relatively short reaction times of the order of tens of seconds or less.[23−33,47−49] The decrease in PL intensity beyond an optimum doping level for samples herein (i.e., at higher dopant levels) is thought to be due to energy transfer between adjacent luminescence centers via cross relaxation.

Conclusions

We report the successful automation and initial operation of a combinatorial robot, the "Rapid Automated Materials Synthesis Instrument", RAMSI, capable of preparing multiple nanocrystal precursor solids (<100 nm) in a sequence that allows the automatic construction of combinatorial libraries. RAMSI was successfully used to form pure yttrium hydrox-

ide and yttrium hydroxide-doped europium nanocrystal precursor solids. An integrated automated cleanup and printing section of RAMSI was used to remove residual counterions and produce ceramic dots which were manually fired to reveal how the different levels of Eu^{3+} doping in yttria affected fluorescence intensities as a function of heat-treatment temperature (and phase behavior) in air. In effect, RAMSI was used to explore both compositional and temperature space for a well-known phosphor system by using a bottom-up approach from the $Y(OH)_3$:Eu^{3+} nanocrystal precursor solids. The approach yielded a novel observation that heat-treatment of such solids and image analysis of the resulting photograph of the samples under broad 254 nm illumination revealed a clear "double hump" contour profile in intensity versus temperature (in the heat-treatment range 200−1200 °C) versus dopant concentration. In particular, samples heat-treated at 500 °C upward, formed Y_2O_3:Eu^{3+} which explains the excellent luminescence of these samples in relation to those heated at lower temperatures. More conclusive studies (e.g., particle size analyses and electron micrographs) will be required to better understand the reasons for this behavior. Finally, the authors believe that such a bottom up and homogeneous synthesis approach as afforded by RAMSI will not only facilitate the rapid development of new phosphors and their ideal processing conditions in the future, but also yield an improved understanding of structure-property-composition relationships.

Acknowledgment. The combinatorial discovery robot RAMSI (Rapid Automated Materials Synthesis Instrument) was named in memory of Sir William Ramsay (FRS) who discovered many of the noble gases in the late 1800s and was Chair of Inorganic Chemistry at University College London (1887−1913) and a Nobel Prize winner in 1904. We are grateful to the Engineering and Physical Sciences Research Council (EPSRC) for funding the "High-Throughput Nanoceramics Discovery Project" under Grants EP/D038499/1 [J.A.D., J.R.G.E., S.K., T.L., K.G.] and EP/D038391/1 [X.W.]. The authors are very much indebted to the staff at Labman Automation of Stokesley, U.K., for the design, building, testing, and reassembly on site of RAMSI which was performed in 2007/08 under contract. In particular we thank A. Whitwell, P. Cooper, J. Marsay, S. Barker, R. Talintyre, P. Chilton, S. Parker, M. Walton, and their support staff. Miss Yang Yang of Leeds University is thanked for the image analysis work associated with the phosphor library. Dr. Bob Keighley of Varian is thanked for measurements using the Cary Eclipse spectrometer.

Supporting Information Available. Details about the equipment, Figures S1−S5, and Table S1. This material is available free of charge via the Internet at http://pubs.acs.org.

References and Notes

(1) O'Regan, B.; Gratzel, M. *Nature* **1991**, *353*, 737.
(2) Brandon, N. P.; Skinner, S.; Steele, B. C. H. *Annu. Rev. Mater. Sci.* **2003**, *33*, 183.
(3) Ge, C.; Xie, C.; Cai, S. *Mat. Sci. Eng., B* **2007**, *137*, 53.
(4) Kaspar, J.; Fornasiero, P. *J. Solid State Chem.* **2003**, *171*, 19.
(5) Evans, J. R. G. *J. Eur. Ceram. Soc.* **2008**, *28*, 1421.
(6) Broach, J. R.; Thorner, J. *Nature* **1996**, *384*, 14.
(7) Archer, R. *Nat. Biotechnol.* **1999**, *17*, 834.
(8) Xiang, X. D.; Sun, X.; Briceto, G.; Lou, Y.; Wang, K. A.; Chang, H.; Wallace-Freedman, W. G.; Chen, S. W.; Schultz, P. G. *Science* **1995**, *268*, 1738.
(9) Pullar, R. C.; Zhang, Y.; Chen, L.; Yang, S.; Evans, J. R. G.; Petrov, P. K.; Salak, A. N.; Kiselev, D. A.; Kholkin, A. L.; Ferreira, V. M.; Alford, N. M. *J. Eur. Ceram. Soc.* **2007**, *27*, 4437.
(10) Pullar, R. C.; Zhang, Y.; Chen, L.; Yang, S.; Evans, J. R. G.; Alford, N. M. *J. Eur. Ceram. Soc.* **2007**, *27*, 3861.
(11) Zhang, Y.; Chen, L.; Yang, S.; Evans, J. R. G. *QSAR Comb. Sci.* **2007**, *26*, 1036.
(12) Yanase, I.; Ohtaki, T.; Watanabe, M. *Solid State Ionics* **2002**, *151*, 189.
(13) Yanase, I.; Ohtaki, T.; Watanabe, M. *Appl. Surf. Sci.* **2002**, *189*, 292.
(14) Fujimoto, K.; Takada, K.; Sasaki, T.; Watanabe, M. *Appl. Surf. Sci.* **2004**, *223*, 49.
(15) Fujimoto, K.; Watanabe, M. *Meas. Sci. Tech.* **2005**, *16*, 41.
(16) Senkan, S. M. *Nature* **1998**, *394*, 350.
(17) Sun, X. D.; Gao, C.; Wang, J.; Xiang, X. D. *Appl. Phys. Lett.* **1997**, *70*, 3353.
(18) Briceto, G.; Chang, H.; Sun, X.; Schultz, P. G.; Xiang, X. D. *Science* **1995**, *270*, 273.
(19) Sun, X. D.; Wang, K. A.; Yoo, Y.; Wallace-Freedman, W. G.; Gao, C.; Xiang, X. D.; Chultz, P. G. *Adv. Mater.* **1997**, *9*, 1046.
(20) Van Dover, R. B.; Schneemeyer, L. F.; Fleming, R. M. *Nature* **1998**, *392*, 162.
(21) Wang, X. Z.; Perston, B.; Yang, Y.; Lin, T.; Darr, J. A. *Chem. Eng. Res. Des.* **2009**, *87* (10A), 1420.
(22) Adschiri, T.; Kanazawa, K.; Arai, K. *J. Am. Ceram. Soc.* **1992**, *75*, 1019.
(23) Darr, J. A.; Poliakoff, M. *Chem. Rev.* **1999**, *99*, 495.
(24) Chaudhry, A. A.; Haque, S.; Kellici, S.; Boldrin, P.; Rehman, I.; Khalid, F. A.; Darr, J. A. *Chem. Commun.* **2006**, 2286.
(25) Weng, X.; Boldrin, P.; Abrahams, I.; Skinner, S. J.; Darr, J. A. *Chem. Mater.* **2007**, *19*, 4382.
(26) Zhang, Z.; Brown, S.; Goodall, J. B. M.; Weng, X.; Thompson, K.; Gong, K.; Kellici, S.; Clark, R. J. H.; Evans, J. R. G.; Darr, J. A. *J. Alloys Compd.* **2008**, *476*, 451.
(27) Weng, X.; Boldrin, P.; Abrahams, I.; Skinner, S. J.; Kellici, S.; Darr, J. A. *J. Solid State Chem.* **2008**, *181*, 1123.
(28) Boldrin, P.; Hebb, A. K.; Chaudhry, A. A.; Otley, L.; Thiebaut, B.; Bishop, P.; Darr, J. A. *Ind. Eng. Chem. Res.* **2007**, *46*, 4830.
(29) Cabanas, A.; Darr, J. A.; Lester, E.; Poliakoff, M. *Chem. Commun.* **2000**, 901.
(30) Zhang, Z.; Goodall, J. B. M.; Morgan, D. J.; Brown, S.; Clark, R. J. H.; Knowles, J. C.; Mordan, N. J.; Evans, J. R. G.; Carley, A. F.; Bowker, M.; Darr, J. A. *J. Eur. Ceram. Soc.* **2009**, *29*, 2343.
(31) Chaudhry, A. A.; Goodall, J.; Vickers, M.; Cockcroft, J. K.; Rehman, I.; Knowles, J. C.; Darr, J. A. *J. Mater. Chem.* **2008**, *18*, 5900.
(32) Middelkoop, V.; Boldrin, P.; Peel, M.; Buslaps, T.; Barnes, P.; Darr, J. A.; Jacques, S. D. M. *Chem. Mater.* **2009**, *21*, 2430.
(33) Weng, X.; Cockcroft, J.; Hyett, G.; Vickers, M.; Boldrin, P.; Tang, C. C.; Thompson, S.; Parker, J. E.; Knowles, J. C.; Rehman, I.; Evans, J. R. G.; Darr, J. A. *J. Comb. Chem.* **2009**, *11*, 829–834.
(34) Lin, T.; Kellici, S.; Gong Kenan; Thompson K.; Evans, J. R. G.; Wang, X. Z.; Darr, J. A. *J. Dalton Trans.* **2009**, manuscript in preparation
(35) Lin, T.; Kellici, S.; Gong, K.; Thompson, K.; Evans, J. R. G.; Wang, X. Z.; Darr, J. A. **2010**, unpublished work.
(36) Das, G. K.; Tan, T. T. Y. *J. Phys. Chem. C* **2008**, *112*, 11211.
(37) Le Bail, A. In *Powder Diffraction Theory and Practice*; Dinnibier, R. E., Billinger, S. J. L., Eds.; RSC: Cambridge, U.K., 2008, 142.

(38) Kang, Y. C.; Roh, H. S.; Park, S. B. *Adv. Mater.* **2000**, *12*, 451.
(39) Konrad, A.; Fries, T.; Gahn, A.; Kummer, F.; Herr, U.; Tidecks, R.; Samwer, K. *J. Appl. Phys.* **1999**, *86*, 3129.
(40) Kottaisamy, M.; Jeyakumar, D.; Jagannathan, R.; Rao, M. M. *Mater. Res. Bull.* **1996**, *31*, 1013.
(41) Gwak, J. H.; Park, S. H.; Jang, J. E.; Lee, S. J.; Jung, J. E.; Kim, J. M.; Jin, Y. W.; Lee, N. S.; Yi, W. K.; Vorobyov, V. A. *J. Vac. Sci. Technol., B: Microelectron. Nanometer Struct.* **2000**, *18*, 1101.
(42) Wakefield, G.; Holland, E.; Dobson, P. J.; Hutchison, J. L. *Adv. Mater.* **2001**, *13*, 1557.
(43) Zhong, S.; Wang, S.; Liu, Q.; Wang, Y.; Wang, S.; Chen, J.; Xu, R.; Luo, L. *Mater. Res. Bull.* **2009**, *44*, 2201.
(44) Zeng, S.; Tang, K.; Li, T.; Liang, Z. *J. Colloid Interface Sci.* **2007**, *316*, 921.
(45) Pang, Q.; Shi, J.; Liu, Y.; Xing, S.; Gong, M.; Xu, N. *Mater. Sci. Eng., B* **2003**, *105*, 57.
(46) Chien, W. C *J. Cryst. Growth* **2006**, *290*, 554.
(47) Thompson, K.; Goodall, J.; Kellici, S.; Mattinson, J. A.; Egerton, T. A.; Rehman, I.; Darr, J. A. *J. Chem. Technol. Biotechnol.* **2009**, *84*, 1717.
(48) Zhang, Z.; Goodall, J. B. M.; Brown, S.; Karlsson, L.; Clark, R. J. H., Hutchison, J. L.; Rehman, I. U.; Darr, J. A.; *Dalton Trans.* **2010**, *39*, 711−714.
(49) Weng, X. L.; Perston, B.; Wang, X. Z.; Abrahams, I.; Lin, T.; Yang, S. F.; Evans, J. R. G.; Morgan, D. J.; Carley, A. F.; Bowker, M.; Knowles, J. C.; Rehman, I.; Darr, J. A. *Appl. Catal., B* **2009**, *90*, 405.

CC9001108